

# Mechanism of HO<sub>x</sub> Formation in the Gas-Phase Ozone–Alkene Reaction. 1. Direct, Pressure-Dependent Measurements of Prompt OH Yields<sup>†</sup>

Jesse H. Kroll,\* James S. Clarke,<sup>‡</sup> Neil M. Donahue,<sup>§</sup> and James G. Anderson

Department of Chemistry and Chemical Biology, Harvard University, Cambridge, Massachusetts 02138

Kenneth L. Demerjian

Department of Earth and Atmospheric Sciences, and Atmospheric Sciences Research Center, SUNY–Albany, Albany, New York 12203

Received: June 12, 2000; In Final Form: October 18, 2000

The gas-phase reaction of ozone with alkenes is known to be a dark source of HO<sub>x</sub> radicals (such as OH, H, and R) in the troposphere, though the reaction mechanism is currently under debate. It is understood that a key intermediate in the reaction is the carbonyl oxide, which is formed with an excess of vibrational energy. The branching ratios of the ozone–alkene reaction products (and thus HO<sub>x</sub> yields) depend critically on the fate of this intermediate: it may undergo unimolecular reaction (forming either OH or dioxirane) or be collisionally stabilized by the bath gas. To investigate this competition between reaction and quenching, we present direct, pressure-dependent measurements of hydroxyl radical (OH) yields for a number of gas-phase ozone–alkene reactions. Experiments are carried out in a high-pressure flow system (HPFS) equipped to detect OH using laser-induced fluorescence (LIF). Hydroxyl radicals are measured in steady state, formed from the ozone–alkene reaction and lost to reaction with the alkene. Short reaction times (usually ~10 ms) ensure negligible interference from secondary and heterogeneous reactions. For all substituted alkenes covered in this study, low-pressure yields are large but decrease rapidly with pressure, resulting in yields at 1 atm which are significantly lower than current recommendations and indicating the important role of collisional stabilization in determining OH yield. The influence of alkene size and degree of substitution on pressure-dependent yield is consistent with the influence of collisional stabilization as well as the accepted reaction mechanism.

## Introduction

The gas-phase reaction of ozone and alkenes has received considerable attention in recent years due to its unique potential as a dark source of tropospheric HO<sub>x</sub> radicals. Over the past decade, numerous indirect scavenger studies<sup>1–8</sup> have provided strong evidence for significant hydroxyl (OH) radical formation from this class of reaction. Recently our laboratory presented the first direct evidence of prompt OH formation, using laser-induced fluorescence to detect OH in the reaction mixture.<sup>9</sup> The amount of hydroxyl radical formed from such reactions is thought to be important in the atmosphere: it has been shown that measured yields are substantial enough to be a significant, even dominant, contributor of total HO<sub>x</sub> in rural and urban environments.<sup>10,11</sup>

The mechanism by which OH is believed to be formed is shown in Figures 1 and 2. Ozone adds to the alkene (reaction R1) to form a vibrationally excited primary ozonide, which quickly dissociates (R2) into a carbonyl oxide (the Criegee intermediate) and a carbonyl species. If the substituents on either side of the alkene double bond are different, this dissociation has two possible sets of products.

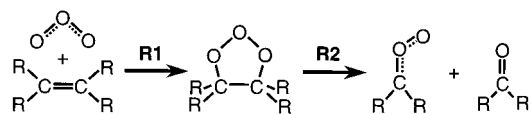


**Figure 1.** Criegee mechanism of carbonyl oxide formation: ozone–alkene cycloaddition (R1) and subsequent dissociation (R2) to form the carbonyl oxide.

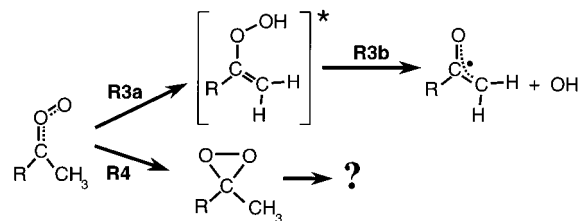


**Figure 2.** Unimolecular reaction channels available to the substituted carbonyl oxide: isomerization (R3a) to an excited hydroperoxide, which will quickly dissociate (R3b) to OH or ring closure to form dioxirane (R4).

The vibrationally excited carbonyl oxide may react via further unimolecular reactions or be collisionally stabilized by the bath gas. There are two primary reaction pathways, dissociation to OH (R3) and ring closure to dioxirane (R4),<sup>12,13</sup> as shown in Figure 2 for a substituted carbonyl oxide. OH formation takes place via an excited hydroperoxide intermediate, which is formed via a five-membered transition state. The fate of the

<sup>†</sup> Part of the special issue “Harold Johnston Festschrift”.

\* Corresponding author. E-mail kroll@fas.harvard.edu.

<sup>‡</sup> Present Address: Laboratorium für Organische Chemie, ETH Zürich, CH-8092 Zürich, Switzerland.

<sup>§</sup> Present Address: Departments of Chemistry and Chemical Engineering, Carnegie Mellon University, Pittsburgh, PA 15213-3890.

dioxirane, which is also formed with excess vibrational energy, is not clear. If the carbonyl oxide is unsubstituted (that is, the methyl group is replaced by an H), OH will form not via a hydroperoxide but rather in a single concerted step. This step occurs via a four-membered transition state and so has a higher barrier to reaction;<sup>14</sup> consequently, the degree of substitution is expected to play an important role in OH yield.

Thus far, most OH yield measurements have relied on the use of a radical scavenger added to the reaction mixture. Most such experiments are performed in environmental chambers, and due to the slow rate of reaction between ozone and alkene, they are carried out over long periods of time, typically several minutes to hours. Thus, unwanted secondary chemistry may interfere. In these studies, OH yield is determined in one of two ways: either from the yield of a product of the OH-scavenger reaction (such as production of cyclohexanone from OH + cyclohexane and cyclohexanol<sup>2,3</sup> or production of CO<sub>2</sub> from OH + CO<sup>1</sup>) or from the decrease in the scavenger concentration.<sup>5,7,8</sup> A third tracer technique, in which OH yield is determined by the change in rate of alkene loss when a scavenger is added to the system, has been recently introduced.<sup>6</sup> In all scavenger studies save one<sup>15</sup> (which is believed to have significantly underestimated experimental error<sup>6,8</sup>), the loss of scavenger or formation of products is consistent with production of OH. Yield results from various studies are generally in good agreement; for a comprehensive list of OH yield measurements see Paulson et al.<sup>8</sup>

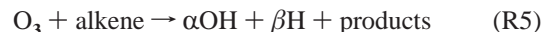
Recently we reported the first direct observation of OH radicals from the ozone–alkene reaction.<sup>9</sup> Radicals were detected using laser-induced fluorescence (LIF) and were measured in steady state, so that no tracer was necessary. In that experiment, OH was detected only 50 ms after reaction initiation, thus minimizing interference by secondary reactions. Formation of OH by secondary reactions could not be entirely ruled out, but prompt formation was suggested by the fact that for one reaction, [OH] remained linear with [O<sub>3</sub>] down to low ozone concentrations. OH production has since been confirmed using a different spectroscopic technique.<sup>16</sup>

While our previous study unequivocally confirmed OH as a product of the ozone–alkene reaction, the pressure range was low (4–6 Torr). In this study we extend the OH yield measurements up to hundreds of Torr, allowing for extrapolation to atmospheric pressures with much less uncertainty. Yields presented here are also considerably more precise than those presented before, and reaction times are significantly shorter, so the influence of secondary reactions is negligible. In addition, in our previous study we reported detecting H atoms by resonance fluorescence (RF); here we have calibrated our RF measurement and therefore present H-atom yields as well.

Our objective is to understand the role of collisional stabilization in OH production, including the influence of substitution on the carbonyl oxide. Consequently, we have selected a series of symmetric alkenes whose reaction pathways are as simple as possible. In all cases only a single carbonyl oxide is produced, though in some cases stereoisomers may play a role. The alkenes in this study are ethene, which produces an unsubstituted carbonyl oxide; *trans*-2-butene, *trans*-3-hexene, and *trans*-4-octene, which produce monosubstituted carbonyl oxides; and 2,3-dimethyl-2-butene (also called tetramethylethylene, or TME) and 3,4-dimethyl-3-hexene, which produce disubstituted carbonyl oxides. As we shall see, this series is sufficient to elucidate and separate the competing roles of size and substitution on collisional stabilization and OH production.

## Experimental Section

As reported previously,<sup>9</sup> we observe radicals in the steady state. OH and H are formed in the ozone–alkene reaction (with yields of  $\alpha$  and  $\beta$ , respectively) and are lost to reaction with the alkene:



When reaction R5 is the sole source and reaction R6 the sole sink of OH, the steady-state concentration of OH is

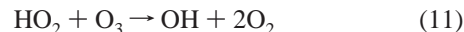
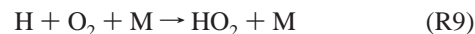
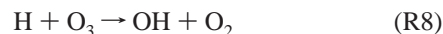
$$[\text{OH}]_{\text{ss}} = \alpha \frac{k_{\text{O}_3}[\text{O}_3]}{k_{\text{OH}}} \quad (1)$$

where OH concentration is linear with ozone concentration but independent of alkene. Therefore, a yield may be obtained by a single ozone and radical measurement. However, it is more precise to take a derivative approach:

$$\alpha = \frac{k_{\text{OH}}}{k_{\text{O}_3}} \frac{\partial[\text{OH}]}{\partial[\text{O}_3]} \quad (2)$$

We take the latter approach in this study, obtaining yields by measuring steady-state radical concentrations at a number of ozone concentrations. This approach is also useful in that it provides a check on our understanding of the OH chemistry: nonlinearities or nonzero intercepts in [OH] versus [O<sub>3</sub>] suggest additional chemistry not included in reactions R5 through R7. The H-atom yield  $\beta$  may be found using steady-state equations similar to eqs 1 and 2.

For the above equations to hold, a number of experimental conditions must be met. The first is that the radicals must be observed in the steady state. Since the alkene serves as the radical sink and thus controls the approach to steady state, this condition can be met by using a high concentration of alkene. In addition, it is necessary that the above reactions (R5–R7) completely describe the chemistry of OH and H in the system. Even in a simple N<sub>2</sub>/O<sub>2</sub>/O<sub>3</sub> environment, there exist numerous additional sources and sinks of OH, including



All of these may be safely neglected so long as all OH and H radicals react with alkene only. Thus, for this study large alkene concentrations and small ozone concentrations are required.

However, this does not necessarily eliminate all interferences from secondary chemistry. Sources of OH (or H) that are independent of [O<sub>3</sub>], such as bimolecular reactions of stabilized intermediates, may still exist. Thus there is the additional requirement that radicals formed via reaction R5 only be formed from unimolecular decomposition of the vibrationally excited intermediates (via reactions 1–4) and not by intermediate bimolecular channels; this may be accomplished by making the experimental time scale as small as possible.

Flow systems, in which experimental time scales are controlled by flow velocity, are well-suited for such measurements. The high-pressure flow system (HPFS) used in this study was

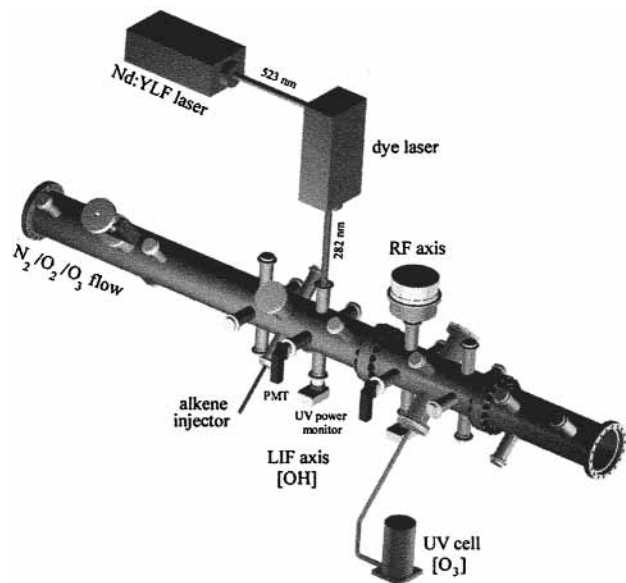


**Figure 3.** The high-pressure flow system (HPFS) used in this study. For H-atom yield measurements, the RF axis is moved upstream (replacing the LIF axis) to ensure the measurement of prompt H formation.

initially designed for measuring rates of radical–molecule reactions,<sup>17</sup> and flow conditions have been extensively analyzed.<sup>18,19</sup> Here major features of the system necessary for yield measurements are outlined. The HPFS is shown in Figure 3; it consists of a stainless steel flow tube, 3.5 m long and 12.36 cm in diameter. The diameter is sufficiently large such that, within the reaction zone, species do not have time to diffuse from the center of the tube to the wall, so that the system is effectively “wall-less”,<sup>19</sup> and thus, potential heterogeneous reactions are categorically eliminated from the observed chemistry. In addition, the  $t = 0$  of the experiment is well-defined, with extremely good time resolution, so that we may make measurements a known time (on the order of milliseconds) after reaction initiation.

Nitrogen is used as the bath gas in this experiment and is regulated by a 400 slm flow controller (MKS). Flow velocity is monitored with a pitot-static tube attached to a 0.2 Torr differential capacitance manometer (MKS) located at the end of the flow tube and is typically 10 m/s. The pressure of the system may be varied from under 1 Torr to an atmosphere; however, pressures over 50 Torr are controlled not by the flow controller but by the valve to the vacuum pump, so that at higher pressures, flow velocities are typically smaller (down to 1 m/s).

Ozone is injected at the beginning of the tube to ensure a uniform radial concentration. Ozone is generated by passing ultrahigh-purity oxygen through a glass tube and subjecting it to a high-voltage electric field. Ozone concentration is modulated by varying the voltage through the oxygen; at maximum voltage ( $\sim 12\,000$  V ac) approximately 7% of the  $O_2$  is converted to  $O_3$ . The  $O_2/O_3$  mixture is then sent into the flow tube at 100 sccm.

Ozone concentration is measured using a UV White cell.<sup>20</sup> A mechanical pump draws gas from the center of the flow tube through  $1/4$  in. Teflon tubing and into the cell. Light from the 254 nm Hg line is multipassed through the cell, for a total path length of 600 cm. The UV cross-section of ozone is well-known at this wavelength ( $1.157 \times 10^{-17}$  cm<sup>2</sup> 21), so a highly precise ozone concentration within the cell may be obtained; this number is then scaled by the ratio of pressure in the HPFS to

pressure in the cell to obtain  $[O_3]$  in the tube. In a separate HPFS, we have compared concentrations obtained using this technique with FTIR measurements;<sup>22</sup> concentrations agree to within a few percent over a wide range of pressures.

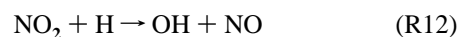
Since this is a bulk sampling technique, measurements cannot be made from within the reaction zone without the risk of interfering with the radical concentrations, spectroscopic measurements, or flows. Thus the UV cell is placed near the end of the tube; this requires that by the time alkene is injected into the flow, the ozone profile has stopped evolving, so that the  $[O_3]$  in the reaction zone equals that further downstream. In other words, the ozone must be of uniform radial concentration; using the UV cell we have verified that in the reaction zone this is the case, over a wide range of experimental conditions.

Alkene is injected into the center of the flow via a quartz injector, located 2.4 m downstream of the beginning of the tube. As mentioned above, high alkene concentrations are generally desired; however, care is taken that flow through the alkene injector is not so high as to interfere with the flat ozone profile (see ref 19). Alkenes used in this study were ethene (99.5+%, Matheson); *trans*-2-butene, 2,3-dimethyl-2-butene, *trans*-3-hexene (all 99+%, Aldrich); 3,4-dimethyl-3-hexene (99+% *cis/trans*, Chemsampco); and *trans*-4-octene (90+%, Aldrich). We do not measure alkene concentration directly, but it may be estimated on the basis of flows through calibrated flow controllers; a typical alkene concentration in the flow tube is  $10^{15}$ – $10^{16}$  molecules/cm<sup>3</sup>.

Hydroxyl radicals are detected using laser-induced fluorescence (LIF), 5–10 cm (corresponding to 5–10 ms) downstream of the alkene injector. While at this point the alkene is a plume, the alkene is well-mixed within the very small volume of the LIF measurement. LIF detection of OH is discussed in ref 23, and its adaptation for the HPFS is described in ref 18. A frequency-doubled, tunable dye laser pumps the  $A^2\Sigma^+ (v = 1) \leftarrow X^2\Pi (v = 0)$  transition in OH (at 282.2 nm). Some of the excited OH fluoresces back to the ground state, but most is collisionally stabilized to the  $v = 0$  state and then fluoresces or is collisionally stabilized to the ground state. This red-shifted fluorescence at 309 nm is measured using a PMT (Hamamatsu) placed normal to the laser beam. A photodiode placed at the end of the beam monitors average UV laser power. The PMT signal, corrected for undercounting<sup>23</sup> and scaled by average power, yields a signal which is proportional to OH number density. The LIF axis used in this experiment is more sensitive than previous HPFS designs, due to better optical filters (Omega Optical) as well as a wider solid angle.

To measure the H-atom yield, we replace the LIF detection axis with a resonance fluorescence (RF) detection axis. Measurement of H atoms in the HPFS is described in detail in ref 17. A sealed lamp consisting of  $UH_3$  in Ne is heated and subjected to an rf plasma, sending Lyman- $\alpha$  (121.6 nm) light into the tube, again normal to the flow. H atoms in the flow absorb the Lyman- $\alpha$  light, and a PMT perpendicular to the lamp monitors the subsequent fluorescence; the fluorescence signal is then scaled by the lamp power, measured by a photodiode opposite the lamp.

Both the LIF and RF have been calibrated by titrating  $NO_2$  in an excess of H atoms:



Trace amounts ( $10^9$ – $10^{11}$ /cm<sup>3</sup>) of  $NO_2$  in the HPFS are maintained in an advective steady state through the addition of a standard  $NO_2/He$  mixture, determined to be 36.4 ppm  $NO_2$  by FTIR spectroscopy. The  $NO_2$  is well-mixed by the time it

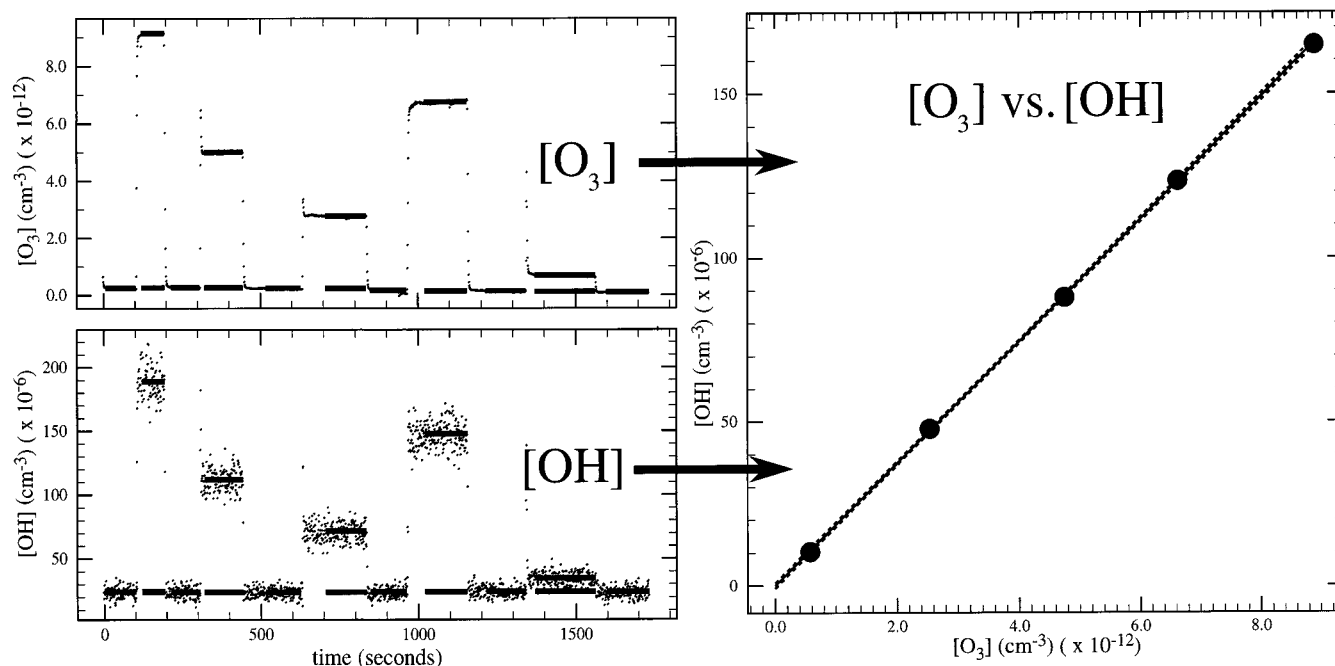


**Figure 4.** Typical run, for ozone + TME at 10 Torr. Ozone is modulated at five different concentrations, with the resultant OH concentration varying accordingly. OH yield is the slope of the [OH] vs [O<sub>3</sub>] line, scaled by  $k_{\text{OH}}/k_{\text{O}_3}$ .

reaches the reaction zone, and its concentration is calculated on the basis of the measured flows. Our H-atom source, described elsewhere,<sup>17</sup> is essentially a H<sub>2</sub>/He/Ar mixture sent through a microwave plasma and injected as a plume into the center of the flow through a quartz injector. We verify that NO<sub>2</sub> is titrated by changing [H] within the plume and finding no change in LIF signal. Calibrations are performed by modulating NO<sub>2</sub> flow (and thus concentration); the calculated NO<sub>2</sub> concentration is equal to loss of H and formation of OH, so we may correlate our change in RF and LIF signals with concentration.

Calibrations have been performed over a range of pressures (5–50 Torr). At high pressures both the RF and LIF calibrations vary with pressure inversely, as expected, since in both cases collisional quenching competes with fluorescence from the excited state. The full pressure dependence of the LIF measurement is understood, and the rates of the individual processes (collisional stabilization vs fluorescence of the excited OH) are known (see ref 23). Our LIF calibration data fit this known pressure dependence well. We have some reason to question the accuracy of our calibration (see Results below), but precision is very high (~10%), and the measured pressure dependences of the yields are reliable. Soon we plan to more accurately calibrate our LIF system by measuring the N<sub>2</sub> Raman shift at 302 nm.<sup>23</sup>

Before a yield measurement is made, a test is done in which ozone and alkene are both injected into the system and alkene flow is modulated. By eq 1, steady-state radical concentration should be independent of alkene concentration, so if the LIF (or RF) signal does not change with a change in alkene flow, the radical is assumed to be in steady state and the yield measurement is performed.

Yield measurements are performed by sending a constant flow of alkene into the reaction zone and modulating ozone on and off at various concentrations. During the “off” cycle the O<sub>2</sub>/O<sub>3</sub> flow is diverted downstream of the UV cell, while background LIF (or RF) and UV signals are taken. In a typical run, this is repeated for four to six ozone concentrations, spanning [O<sub>3</sub>] by

at least a factor of 3 and often a factor of 10 or more. A yield measurement for a given alkene and pressure takes between 10 and 45 min.

Because of the reduced sensitivity of LIF and RF at high pressures (>50 Torr), higher concentrations of ozone, and therefore alkene, are often used. Also in these cases, as well as at low pressures (<3 Torr), velocity can be slower as well. Therefore it is possible that a significant fraction of the ozone will have reacted between the reaction zone and the UV cell. To compensate for this, we measure ozone concentrations without alkene and use these values for calculating the yield; this correction is generally of the order of a few percent and is never higher than 15%.

## Results

A typical run, for TME at 10 Torr, is shown in Figure 4. Ozone is held at five different concentrations, and the resulting OH signal is proportional to ozone concentration. The detection of OH is unequivocal; detuning the laser reveals the 3:1 doublet characteristic of the OH transition. Laser-generation of OH, by photolysis of O<sub>3</sub> to O(<sup>1</sup>D) followed by H-atom abstraction, is a potential problem, but our experimental design greatly minimizes this interference. We draw on the proven design of the NASA ER2 HO<sub>x</sub> instrument,<sup>23</sup> using very high laser pulse repetition rates to keep the peak laser power (and thus secondary production) low. Two separate tests have established that none of the OH observed is laser-generated. First, measured OH yield is independent of laser power, suggesting that no two-photon processes (namely ozone photodissociation and subsequent OH detection) are occurring. Second, negligible LIF signal is observed when a large amount of isobutane is added to the ozone in the system. Isobutane has a tertiary hydrogen and thus is expected to be significantly more susceptible to H-atom abstraction than any of the alkenes used in this study. We thus conclude that laser-generated OH does not interfere with our experiment.

Plotting [OH] vs [O<sub>3</sub>] shows an extremely tight correlation, as predicted by the steady-state expression (eq 2). The yield, as

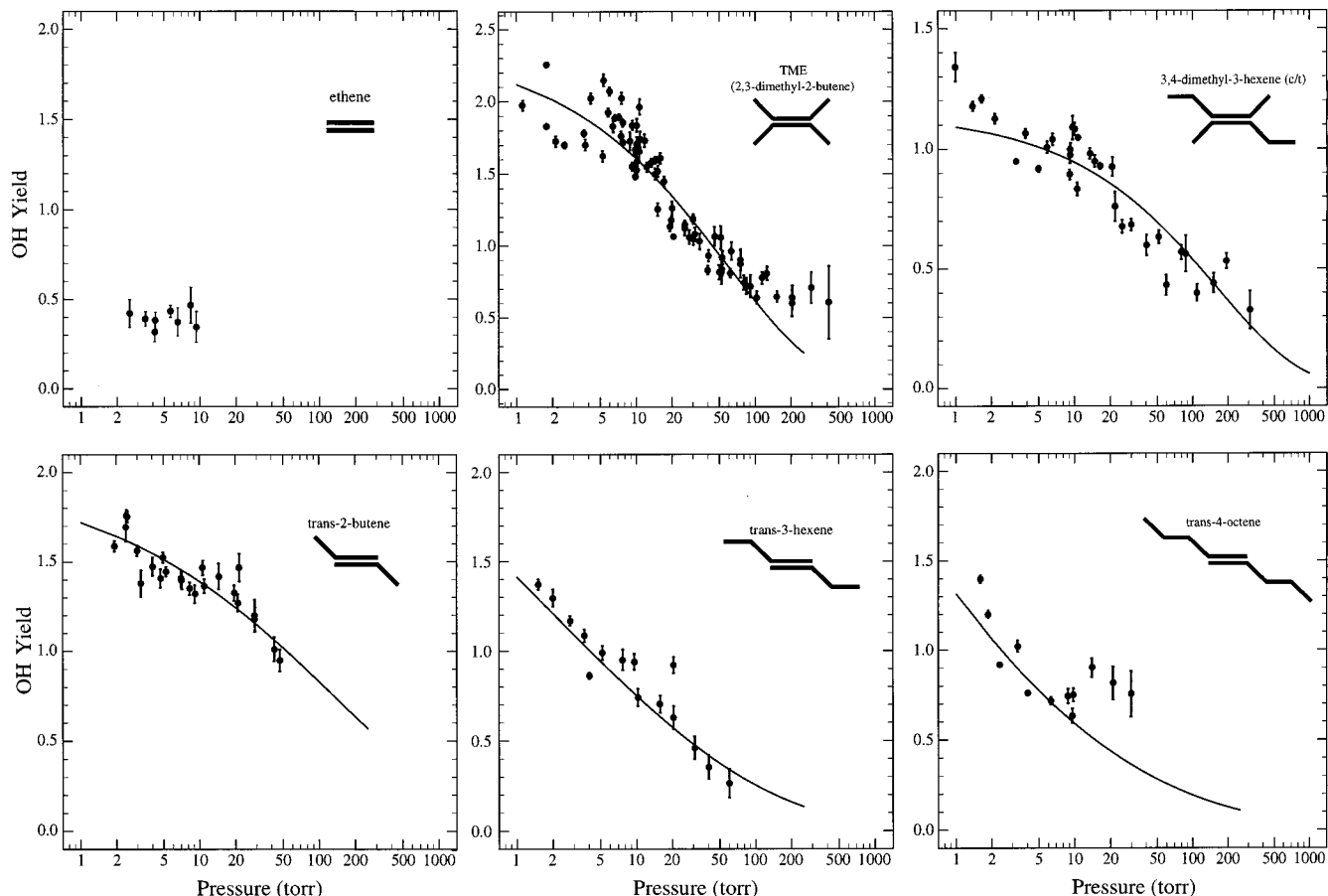


**Figure 5.** OH yields versus pressure (in Torr) for the six alkenes covered in this study. Data are fit to an empirical function which duplicates master equation results well; yields may be greater than 1 due to uncertainties in  $k_{\text{OH}}$ ,  $k_{\text{O}_3}$ , and LIF calibration (see text).

determined by the slope of the line multiplied by  $k_{\text{OH}}/k_{\text{O}_3}$ , is 1.86. The measured yield above unity is probably not real but instead caused by errors in  $k_{\text{OH}}$ ,  $k_{\text{O}_3}$ , or the LIF calibration, all of which scale the raw data. Such errors do not affect the precision of the measurements, nor do they significantly affect the reported pressure dependence of the yields: as mentioned above, the pressure dependence of LIF sensitivity is well-constrained. Uncertainties in the pressure dependences of the rate constants ( $k_{\text{OH}}$ ,  $k_{\text{O}_3}$ ) may be a factor, but there is little evidence that those rates are significantly pressure-dependent. An important exception is the reaction of OH with ethene, but the pressure dependence of that reaction is well-characterized.<sup>24</sup>

We have found that  $[\text{OH}]$  remains linear with  $[\text{O}_3]$  as low as  $10^{11}$  molecules  $\text{O}_3/\text{cm}^3$ . This demonstrates that the OH is indeed a prompt product of the reaction and is not formed by secondary processes: the lifetime of a species which reacts at the collision rate ( $k = 3 \times 10^{-10}$   $\text{cm}^3 \text{ molecule}^{-1} \text{ s}^{-1}$ ) with ozone or a reaction product (with concentration of  $\leq 10^{11}$  molecules/ $\text{cm}^3$ ) is 33 ms, longer than the time scale of the experiment. Furthermore, bimolecular rate constants for carbonyl oxides are believed to be much slower than the collision rate;<sup>24</sup> secondary reactions with ozone or reaction products are thus not significant in this experiment. Our alkene concentration ( $10^{15}$ – $10^{16}/\text{cm}^3$ ) is much higher than  $[\text{O}_3]$ , so secondary reactions with the alkene are at least possible on the time scale of our experiment. However, this is unlikely to lead to any interference, as there are few alkene reactions that could produce OH; those that might (such as reactions with  $\text{HO}_2$ , or carbonyl oxide + alkene cycloadditions) have high barriers and thus long time scales well beyond that of our experiment. We also cannot completely rule out

**TABLE 1: Rate Constants for Reactions of Alkenes with  $\text{O}_3$ , OH, and  $\text{H}^a$**

| alkene                 | $k_{\text{O}_3}/(10^{-17})$ | $k_{\text{OH}}/(10^{-12})$ | $k_{\text{H}}/(10^{-12})$ |
|------------------------|-----------------------------|----------------------------|---------------------------|
| ethene                 | 0.159( $\pm 0.048$ )        | p-dep <sup>b</sup>         | p-dep <sup>c</sup>        |
| <i>trans</i> -2-butene | 19( $\pm 6.7$ )             | 64.0( $\pm 12.8$ )         | 0.825( $\pm 0.006$ )      |
| TME                    | 113( $\pm 40$ )             | 110( $\pm 22$ )            | 1.34( $\pm 0.010$ )       |
| <i>trans</i> -4-octene | 13( $\pm 1.5$ )             | 69( $\pm 17$ )             | na                        |
| 3,4-dimethyl-3-hexene  | 37                          | na                         | 1.05( $\pm 0.006$ )       |

<sup>a</sup> Values for  $k_{\text{OH}}$  and  $k_{\text{O}_3}$  are from ref 1 and  $k_{\text{H}}$  are from ref 17. Rates are in molecules/ $\text{cm}^3/\text{s}$ ; "na" indicates no value is available. <sup>b</sup> Pressure-dependent rate constant, from ref 24. <sup>c</sup> Pressure-dependent rate constant, from ref 17.

bimolecular reactions with  $\text{O}_2$ , which is present in higher concentrations than  $\text{O}_3$ ; however, by varying  $[\text{O}_2]$  we see no change in the measured yield.

Table 1 presents the values of the rate constants used for determining yield;  $k_{\text{OH}}$  and  $k_{\text{O}_3}$  are from the recommendations in ref 24 and  $k_{\text{H}}$  are from the values determined in this laboratory, presented in ref 17. For the six alkenes in this study, two  $k_{\text{OHS}}$  (*trans*-3-hexene and 2,3-dimethyl-3-hexene) and two  $k_{\text{HS}}$  (*trans*-3-hexene and *trans*-4-octene) have not been measured; in these cases we approximate the  $k_{\text{OH}}/k_{\text{O}_3}$  or  $k_{\text{H}}/k_{\text{O}_3}$  ratio as that for *trans*-2-butene or TME, depending on the level of alkene substitution.

Pressure-dependent OH yields for the six alkenes in this study are shown in Figure 5. The fact that for most alkenes maximum yields exceed unity suggests that the LIF calibration is imperfect; however, errors in rate constants may also contribute. Data are fit to the empirical function  $\text{yield}(P) = a_0 \exp[-a_1 P^{a_2}]$  (in which  $a_0$ ,  $a_1$ , and  $a_2$  are adjustable parameters), which we have found

TABLE 2: OH Yields as Measured by Scavenger Studies at 1 Atm

| study                          | ethene            | <i>trans</i> -2-butene | <i>trans</i> -3-hexene | TME               |
|--------------------------------|-------------------|------------------------|------------------------|-------------------|
| Atkinson et al. <sup>1,2</sup> | 0.12(+0.06/−0.04) | 0.64(+0.32/−0.21)      |                        | 1.00(+0.50/−0.33) |
| Chew and Atkinson <sup>3</sup> |                   |                        |                        | 0.80(±0.12)       |
| Gutbrod et al. <sup>4</sup>    | 0.08(±0.01)       | 0.24(±0.02)            |                        | 0.36(±0.02)       |
| Rickard et al. <sup>5</sup>    | 0.14(±0.07)       | 0.54(±0.14)            |                        | 0.89(±0.22)       |
| Paulson et al. <sup>7,8</sup>  | 0.18(±0.06)       | 0.64                   | 0.47(±0.07)            | 1.00              |

TABLE 3: Low-Pressure Hydrogen Atom Yields

| alkene                 | yield           |
|------------------------|-----------------|
| ethene                 | 0.076 ± 0.060   |
| <i>trans</i> -2-butene | 0.045 ± 0.0028  |
| <i>trans</i> -3-hexene | 0.021 ± 0.0041  |
| <i>trans</i> -4-octene | 0.0072 ± 0.0026 |
| TME                    | 0.0022 ± 0.0010 |
| 3,4-dimethyl-3-hexene  | 0.0024 ± 0.0021 |

fits master equation results well (we discuss our use of the master equation in a separate paper<sup>25</sup>). For the fit, data points are weighted by their respective uncertainties.

Measurements of OH yields for ethene above 10 Torr were not made due to very low precision: when pressure is increased, not only does LIF sensitivity decrease but the OH–ethene rate constant ( $k_{\text{OH}}$ ) increases, decreasing the steady-state concentration of OH.

Due to the poor signal-to-noise ratio, H-atom yields are determined at low pressures: 10 Torr for the substituted alkenes and 5 Torr for ethene. Results are presented in Table 3. For all alkenes, yields are small but nonzero; in general, yield decreases with size and degree of substitution.

## Discussion

For the reaction of ozone with all the alkenes studied, OH is found to be produced promptly. In all cases save ethene, yields are found to be highly pressure-dependent, indicating competition between collisional stabilization and dissociation of a vibrationally excited intermediate, presumably the carbonyl oxide. This conclusion is supported by the fact that the data are generally fit well by our empirical function; one notable exception is the high-pressure TME data.

Given the competition between stabilization and dissociation, we would expect that the larger alkenes (those with more vibrational modes) would exhibit the greatest pressure dependence, as they are the most susceptible to collisional stabilization. Within the series of alkenes studied, this effect seems to be weak but existent: *trans*-2-butene, for example, certainly exhibits a weaker pressure dependence than *trans*-4-octene. Yields from larger alkenes (including many species which are important in the troposphere) are expected to be even more strongly pressure-dependent.

As is to be expected, OH yield is closely related to degree of alkene substitution. TME is found to have the highest yields, consistent with the reaction mechanism shown in Figure 2, in which OH is formed via the hydroperoxide channel. On the other hand, ethene is found to have the lowest yields, consistent with isomerization to dioxirane dominating over dissociation to OH. The three disubstituted alkenes (*trans*-2-butene, *trans*-3-hexene, and *trans*-4-octene) may react by either mechanism, and correspondingly their OH yields are intermediate.

However, while the degree of substitution may control absolute yields, it does not seem to have a significant influence on the pressure dependences of such yields. The degree of substitution affects not only which reaction pathways are available but also the stability of the carbonyl oxide, since alkyl groups serve to stabilize the electron-poor carbon. For two

alkenes with the same number of vibrational modes but different degree of substitution (for example, TME and *trans*-3-hexene), the observed pressure dependences are not drastically different, even though the disubstituted carbonyl oxide (from TME) is significantly more stable than the monosubstituted one. This suggests that only the excess energy of the ozonide—which is not expected to vary much from reaction to reaction—determines the vibrational energy content of the carbonyl oxide.

In addition, we present the first direct measurements of H-atom yields from gas-phase ozonolysis. The H yields are extremely small (<1%) for the fully substituted alkenes (TME and 3,4-dimethyl-3-hexene), which is consistent with the hydroperoxide channel being the dominant reaction mechanism. For ethene, H yield is larger (at low pressures at least), on the order of a few percent. This suggests an alternate reaction mechanism; one possible source is the “hot acid” channel,<sup>26</sup> in which the dioxirane isomerizes to highly excited formic acid, via a dioxymethane intermediate. This acid can then dissociate to one of many sets of products, including H atoms; the observed H may also arise from the dissociation of HCO. For the disubstituted alkenes, H yields are small but not insignificant, ranging from 4.5% for *trans*-2-butene to 0.7% for *trans*-4-octene. This too may be from dissociation of the “hot acid,” to form H + RCO<sub>2</sub>. However, the observed H may be formed instead via the hydroperoxide channel (reaction R6b): the resulting HCOCR<sub>2</sub> fragment may further dissociate, to a ketene and an H atom.

Table 2 presents a summary of OH indirect yield measurements, made at 1 atm. With the exception of ethene, extrapolation of the data in this study to 1 atm suggests OH yields significantly lower than those determined in most scavenger studies. Recently, the Paulson laboratory has determined ethene OH yields to be pressure-dependent, with significantly higher yields at pressures below 100 Torr.<sup>27</sup> Because of the limited pressure range of our measurements, as well as the large error bars in our calculations, we cannot rule out the possibility of a pressure dependence. However, the same study reports no pressure dependence for *trans*-2-butene, *trans*-3-hexene, or TME,<sup>27</sup> in sharp contrast with the results of this work.

It is of course extremely important to understand the source of this discrepancy. An obvious candidate is the different method of OH detection: direct, spectroscopic detection versus indirect, scavenger-based measurements. But this is unlikely to introduce any major errors, as the measurements in scavenger studies are most certainly of OH and not some other oxidant. Thus the difference likely lies in an additional source of OH, not present in our system but present in the scavenger studies.

This additional source may arise from generation of OH via secondary chemistry in the scavenger studies that could not occur within the time scale of our experiments. OH has been suggested as a possible product of the reaction of carbonyl oxide with carbonyls<sup>28</sup> or water.<sup>29,30</sup> In addition, RO<sub>2</sub> chemistry is highly uncertain and may also be an OH source, via either unimolecular or bimolecular channels. Still, there is little evidence that any of these potential sources could produce enough OH to account for the large differences in yields measured in this study and in scavenger studies.

In another paper<sup>25</sup> in this series, we present an alternate explanation for this discrepancy, using the time-dependent master equation. We show that the carbonyl oxide, assuming it does not undergo fast bimolecular reactions, may dissociate to OH thermally on the time scales of the scavenger studies, but not of our experiments.

### Conclusions

We have presented spectroscopic measurements of OH yields from the gas-phase ozone–alkene reaction for a series of simple, symmetric alkenes over a wide range of pressures. These constitute the first direct gas-phase OH measurements from this class of reaction at pressures above a few Torr. In all cases we observe prompt OH formation, and in all cases (save ethene) the yield is pressure-dependent. This is consistent with a competition between unimolecular reaction and collisional stabilization of the vibrationally excited carbonyl oxide intermediate. As expected, the larger alkenes exhibit a greater pressure dependence, but this effect is not particularly strong. The relationship between yield and degree of substitution is more pronounced, suggesting our understanding of the reaction mechanism (reactions R1–R4) is qualitatively accurate, even if the branching ratios are not well constrained. In another paper<sup>25</sup> we use statistical-dynamical calculations to estimate these branching ratios, further constraining the reaction mechanisms. Yields of H atoms were also measured directly for the first time, and may be understood in terms of the “hot acid” channel, available only for ethene and disubstituted alkenes. Finally, for the substituted alkenes, our measured yields, extrapolated to 1 atm, are considerably lower than those determined by scavenger studies; this point, too, will be addressed in the companion paper.

**Acknowledgment.** This work was supported by US EPA STAR grant R825258010 (University at Albany-SUNY and Harvard University), as well as NSF grant 9414983 (Harvard University). J.H.K. gratefully acknowledges support from the NSF Graduate Student Fellowship program.

### References and Notes

- (1) Atkinson, R.; Aschmann, S. M.; Arey, J.; Shorees, B. *J. Geophys. Res.* **1992**, *97*, 6065.
- (2) Atkinson, R.; Aschmann, S. M. *Environ. Sci. Technol.* **1993**, *27*, 1357.
- (3) Chew, A. A.; Atkinson, R. *J. Geophys. Res.* **1996**, *101*, 28649.
- (4) Gutbrod, R.; Meyer, S.; Rahman, M. M.; Schindler, R. N. *Int. J. Chem. Kinet.* **1997**, *29*, 717.
- (5) Rickard, A. R.; Johnson, D.; McGill, C. D.; Marston, G. *J. Phys. Chem. A* **1999**, *103*, 7656.
- (6) Neeb, P.; Moortgat, G. K. *J. Phys. Chem. A* **1999**, *103*, 9003.
- (7) Paulson, S. E.; Fenske, J. D.; Sen, A. D.; Callahan, T. W. *J. Phys. Chem. A* **1999**, *103*, 2050.
- (8) Paulson, S. E.; Chung, M. Y.; Hassan, A. S. *J. Phys. Chem. A* **1999**, *103*, 8125.
- (9) Donahue, N. M.; Kroll, J. H.; Anderson, J. G.; Demerjian, K. L. *Geophys. Res. Lett.* **1998**, *25*, 59.
- (10) Paulson, S.; Orlando, J. *Geophys. Res. Lett.* **1996**, *23*, 3727.
- (11) Ariyam, P. A.; Sander, R.; Crutzen, P. J. *J. Geophys. Res.* **2000**, *105*, 17721.
- (12) Martinez, R. I.; Herron, J. T.; Huie, R. E. *J. Am. Chem. Soc.* **1981**, *103*, 3807.
- (13) Niki, H.; Maker, P. D.; Savage, C. M.; Breitenbach, L. P.; Hurley, M. D. *J. Phys. Chem.* **1987**, *91*, 941.
- (14) Gutbrod, R.; Schindler, R. N.; Kraka, E.; Cremer, D. *Chem. Phys. Lett.* **1996**, *252*, 221.
- (15) Schäfer, C.; Horie, O.; Crowley, J. M.; Moortgat, G. K. *Geophys. Res. Lett.* **1997**, *24*, 1611.
- (16) Pfeiffer, T.; Forberich, O.; Comes, F. J. *Chem. Phys. Lett.* **1998**, *298*, 351.
- (17) Clarke, J. S.; Donahue, N. M.; Kroll, J. H.; Rypkema, H. A.; Anderson, J. G. *J. Phys. Chem.* **2000**, *104*, 5254.
- (18) Abbatt, J. P. D.; Demerjian, K. L.; Anderson, J. G. *J. Phys. Chem.* **1990**, *94*, 4566.
- (19) Donahue, N. M.; Clarke, J. S.; Demerjian, K. L.; Anderson, J. G. *J. Phys. Chem.* **1996**, *100*, 5821.
- (20) Weinstock, E. M.; Schiller, C. M.; Anderson, J. G. *Geophys. Res. Lett.* **1986**, *91*, 5237.
- (21) DeMore, W. B.; Sander, S. P.; Golden, D. M.; Hampson, R. F.; Kurylo, M. J.; Howard, C. J.; Ravishankara, A. R.; Kolb, C. E.; Molina, M. J. Chemical kinetics and photochemical data for use in stratospheric modeling. Technical Report 97-4, Jet Propulsion Laboratory, 1997.
- (22) Donahue, N. M.; Demerjian, K. L.; Anderson, J. G. *J. Phys. Chem.* **1996**, *100*, 17855.
- (23) Wennberg, P.; Cohen, R. C.; Hazen, N. L.; Lapson, L. B.; Allen, N. T.; Hanco, T. F.; Oliver, J. F.; Lanham, N. W.; Demusz, J. N.; Anderson, J. G. *Rev. Sci. Instr.* **1994**, *65*, 1858.
- (24) Calvert, J. G.; Atkinson, R.; Kerr, J. A.; Madronich, S.; Moortgat, G. K.; Wallington, T. J.; Yarwood, G. *The Mechanisms of Atmospheric Oxidation of the Alkenes*. Oxford University Press: New York, 2000.
- (25) Kroll, J. H.; Sahay, S. R.; Anderson, J. G.; Demerjian, K. L.; Donahue, N. M. *J. Phys. Chem. A*, submitted.
- (26) Herron, J. T.; Huie, R. E. *J. Am. Chem. Soc.* **1977**, *99*, 5430.
- (27) Fenske, J. D.; Hasson, A. S.; Paulson, S. E.; Kuwata, K. T.; Ho, A.; Houk, K. N. *J. Phys. Chem. A* **2000**, *104*, 7821.
- (28) Neeb, P.; Horie, O.; Moortgat, G. K. *J. Phys. Chem. A* **1998**, *102*, 6778.
- (29) Paulson, S. E.; Flagan, R. C.; Seinfeld, J. H. *Int. J. Chem. Kinet.* **1992**, *23*, 103.
- (30) Neeb, P.; Sauer, F.; Horie, O.; Moortgat, G. K. *Atmos. Environ.* **1997**, *31*, 1417.